

TWO-DIMENSIONAL DIRECT NUMERICAL SIMULATION OF OPPOSED-JET HYDROGEN/AIR FLAMES: TRANSITION FROM A DIFFUSION TO AN EDGE FLAME

J. LEE,¹ C. E. FROUZAKIS² AND K. BOULOCHOS¹

¹*Swiss Federal Institute of Technology Zurich (ETHZ)
Zurich, CH-8092, Switzerland*

²*Combustion Research Section
Paul Scherrer Institute
Villigen, CH-5232, Switzerland*

In an opposed-jet diffusion flame experiment, under certain conditions, after the extinction of the diffusion flame, an edge flame can be obtained. This ring-shaped edge flame was first reported in 1959 by Potter and Butler but received little attention. It was reported again recently in a numerical and an experimental work and is responsible for an interesting transition between two distinct burning flames (multiple solutions). Motivated by our previous numerical results, obtained with simplified kinetics and some recently reported experimental data, we performed direct numerical simulations of this transition to investigate the underlying physical mechanisms. The appearance of an edge flame after the extinction of the diffusion flame, the hysteresis reported in the experiments, and the existence of multiple vigorously burning flames at identical conditions are all captured by our simulations. Our numerical results show that, in the absence of an inert coflow curtain, when the diffusion flame disk is extinguished, an edge flame forms and propagates in the mixing layer. After the formation of this edge flame, even when the applied strain rate is reduced to the initial subcritical value, the diffusion flame disk does not reappear, because the local fluid velocity still exceeds the propagation speed of the edge flame. This hysteresis has significant implications in the common submodel that utilizes the strain rate as a parameter to determine local reignition in flamelet models; it indicates that a subcritical strain rate is not a sufficient condition for the reignition of a diffusion flame. Further investigation of this phenomenon is clearly needed to refine submodels of local extinction and reignition in the flamelet models for turbulent diffusion flames. The opposed-jet configuration provides a convenient platform to analyze edge flames which are stabilized aerodynamically in a two-dimensional geometry, thus making matching two-dimensional direct numerical simulations effective.

Introduction

We report direct numerical simulations (DNSs) of a transition of flame configuration recently reported in the experiments of Pellett et al. [1] on a diffusion flame of diluted hydrogen and air stabilized on an opposed-jet burner. A similar phenomenon was reported in one of our early papers [2], where we analyzed the effects of the Damköhler number on the flame configuration in an opposed-jet geometry. In fact, as early as 1959, in the pioneering work of Potter and Butler [3], such a ring-shaped edge flame was observed; it was then called the “broken” flame. Even though the opposed-jet configuration is used extensively in studying strained diffusion flames, the transition involving an edge flame is rarely reported, primarily because such edge flames exist after the local extinction of the strained diffusion flame only when there is no inert gas coflow curtain—a very

common practice in experiments to reduce the effects of air entrainment and buoyancy and to eliminate the “edge” of the flame in order to create a disk-shaped flame and facilitate laser diagnostics.

Tomboulides et al. [2] reported a two-dimensional simulation of an opposed-jet diffusion flame using one-step chemistry and simplified transport properties without the inert coflow curtain. It was found that when the Damköhler number was increased beyond a critical value, the flame structure changed from a disk-shaped diffusion flame to an edge flame. It was shown that the edge flame was a tribrachial, or triple, flame with rich and lean premixed arms and a trailing diffusion flame. In Ref. [1], the large hysteresis between “blowoff” and “restoration” (terminology of Ref. [1]) and, in particular, the description of the ring-shaped flame resemble what was reported in Ref. [2]. We suspect the underlying physical mechanism for the phenomena observed in

Report Documentation Page				Form Approved OMB No. 0704-0188	
Public reporting burden for the collection of information is estimated to average 1 hour per response, including the time for reviewing instructions, searching existing data sources, gathering and maintaining the data needed, and completing and reviewing the collection of information. Send comments regarding this burden estimate or any other aspect of this collection of information, including suggestions for reducing this burden, to Washington Headquarters Services, Directorate for Information Operations and Reports, 1215 Jefferson Davis Highway, Suite 1204, Arlington VA 22202-4302. Respondents should be aware that notwithstanding any other provision of law, no person shall be subject to a penalty for failing to comply with a collection of information if it does not display a currently valid OMB control number.					
1. REPORT DATE 04 AUG 2000		2. REPORT TYPE N/A		3. DATES COVERED -	
4. TITLE AND SUBTITLE Two-Dimensional Direct Numerical Simulation of Opposed-Jet Hydrogen/Air Flames: Transition from a Diffusion to an Edge Flame				5a. CONTRACT NUMBER	
				5b. GRANT NUMBER	
				5c. PROGRAM ELEMENT NUMBER	
6. AUTHOR(S)				5d. PROJECT NUMBER	
				5e. TASK NUMBER	
				5f. WORK UNIT NUMBER	
7. PERFORMING ORGANIZATION NAME(S) AND ADDRESS(ES) Swiss Federal Institute of Technology Zurich (ETHZ) Zurich, CH-8092, Switzerland				8. PERFORMING ORGANIZATION REPORT NUMBER	
9. SPONSORING/MONITORING AGENCY NAME(S) AND ADDRESS(ES)				10. SPONSOR/MONITOR'S ACRONYM(S)	
				11. SPONSOR/MONITOR'S REPORT NUMBER(S)	
12. DISTRIBUTION/AVAILABILITY STATEMENT Approved for public release, distribution unlimited					
13. SUPPLEMENTARY NOTES See also ADM001790, Proceedings of the Combustion Institute, Volume 28. Held in Edinburgh, Scotland on 30 July-4 August 2000.					
14. ABSTRACT					
15. SUBJECT TERMS					
16. SECURITY CLASSIFICATION OF:			17. LIMITATION OF ABSTRACT UU	18. NUMBER OF PAGES 6	19a. NAME OF RESPONSIBLE PERSON
a. REPORT unclassified	b. ABSTRACT unclassified	c. THIS PAGE unclassified			

Ref. [1] is the formation and propagation (with positive propagation velocity) of an edge flame. Unfortunately, no further information on the structure of the edge flame, such as flame shape visualization, temperature, and so forth, are available in Ref. [1]. The similarity between the experimental findings [1] and our earlier numerical results [2], the novelty of using an opposed-jet setup to study edge flames, and its implications on the modeling of extinction and reignition of a diffusion flamelet [4,5] prompted us to investigate this diffusion/edge flame transition further using detailed two-dimensional transient simulations with conditions that match those used in the experiment.

In general, an edge flame exists on the boundary of a diffusion flame. Depending on the sign of its propagation velocity, it can be an ignition wave or a failure wave [6]. However, unlike a premixed flame, the propagation speed of an edge flame is dependent on many parameters in addition to the thermodynamic properties (including kinetics and transport properties) of the mixture. Its ability to propagate with a positive or negative velocity is responsible for the spread or blowout of a diffusion flame. It also offers the mechanism for a diffusion flame to anchor itself [6–11]. Since an edge flame exists whenever a diffusion flame has a boundary (such as a hole on a diffusion flame sheet), it is known to play an important role in turbulent diffusion flames, as it is responsible for the local phenomena of extinction (failure wave) and reignition (ignition wave) [4,10,12]. The triple flame, a special case of edge flames, has received considerable attention. For example, the theoretical work of Dold [13] and Hartley and Dold [14], the one-dimensional model of Buckmaster [6], the experimental/numerical work of Kioni et al. [15], and the numerical work of Ruetsch et al. [16] all illustrate that the propagation velocity of the triple flame depends on the transverse gradient of the mixture concentration, flame curvature, and transport in the transverse direction. Two-dimensional numerical simulations of triple flames in the coflow geometry for both the transient and steady (burner stabilized) cases with chemical kinetics and transport models of various complexities have recently been reported [17–20].

In this paper, we focus on the multiple vigorously burning (as opposed to the weakly burning or pure mixing solution) stable flames observed in an opposed-jet configuration [1]. We perform calculations with conditions that match one set of experimental conditions to investigate the nature of the two different flames. In particular, we are interested in showing that an edge flame is indeed responsible for what was observed in Ref. [1] and in providing additional information on the structure of this edge flame. Note that the multiple solution phenomenon considered here is unlike the familiar S-shaped curve with the upper branch representing a burning

flame and the lower branch corresponding to pure mixing (or a weakly burning solution) [6]. We observed two stable flames in addition to the pure mixing solution—that is, three stable solutions. To the best of our knowledge, this is the first attempt to perform DNSs of multiple vigorously burning solution branches and the associated hysteresis effects. Finally, we would like to note that in using the opposed-jet geometry, we were able to simulate three different types of edge flames: a propagating ignition wave (positive propagation velocity with respect to the unburned stream), a propagating failure wave (negative propagation velocity with respect to the unburned stream), and also the flame structure at the edge of the diffusion flame disk. Due to the length limitation on the symposium papers, these other edge flames will be reported elsewhere in the near future.

Methodology and Problem Definition

We employed a direct numerical simulation approach to solve the transient, two-dimensional, low Mach number reduced form of the conservation equations of mass, momentum, energy, and species in the axisymmetric cylindrical coordinate system. The numerical code employed is based on the spectral element method for spatial discretization and a high-order stiffly stable splitting scheme that separates the thermochemistry from the hydrodynamic subsystems for time integration. A special method was employed to ensure exponential convergence on the axis of symmetry [21]. Details on the mathematical formulation and the numerical method can be found in Refs. [2,22], while some of our previous studies with this numerical code can be found in Refs. [23,24]. Recently, we implemented the matrix-free stiff ordinary differential equation solver VODEPK [25], which solves the thermochemistry part much more efficiently than the previous solver (LSODES [26]).

Detailed chemical kinetics [27] and realistic transport (the mixture fraction formulation with a correction diffusion velocity term to preserve the conservation of mass [28]) were utilized in the simulations. Grid independence was ensured by repeating calculations with increasing orders of interpolants, and the minor effect of the outflow boundaries on the solution was verified by placing them at increasing distance from the axis of symmetry. The solutions presented here were obtained on a numerical grid with spatial resolution (in the flame region) better than 0.02 mm, which is adequate to resolve flames in the H₂/air system. We utilized accurate time integration to simulate the actual procedure employed in the experiment to produce multiple vigorously burning flames.

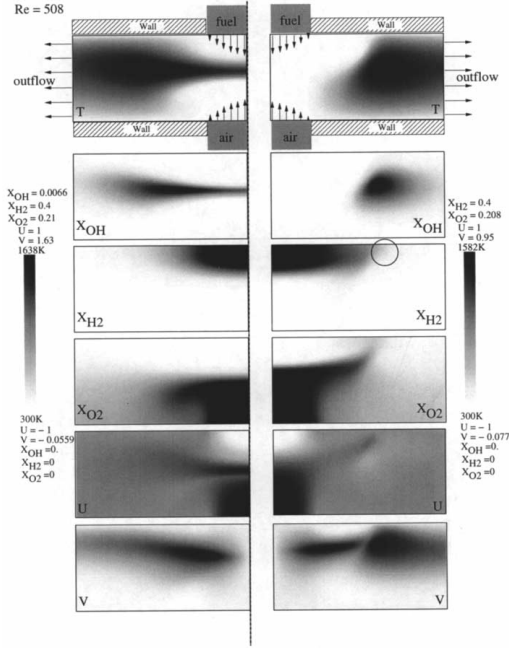


FIG. 1. Isocontours of velocity components, temperature, and mole fraction of selected species. Left column, a contiguous diffusion flame; right column, an edge flame. $Re = 508.8$ in both cases; also, the numerical domain is truncated in the radial direction. Because of the axial symmetry, only half of the numerical domain is shown (the numerical domain on the right is the mirror image of that on the left).

The geometry was that of an axially symmetric opposed-jet burner, with fuel and air nozzles of diameter $D = 0.27$ cm placed at a distance of $L = 0.27$ cm apart. The numerical domain was large (the outflow boundary was placed three diameters away from the nozzles) to accommodate the edge flame, which was found at positions away from the axis of symmetry. The geometry of the numerical domain was simply a rectangle, similar to that reported in Ref. [24]. The upper and lower boundaries of the numerical domain (Fig. 1) were assumed to be non-reactive walls of constant temperature (fixed at 300 K). The flux of species through these walls was zero, and the no-slip boundary condition was enforced. Zero-Neumann boundary condition was applied at the outflow boundary. We are aware that in the experiment reported in Ref. [1], there was no cold wall, and air entrainment would further dilute the mixture in the boundary. We chose a cold wall as our numerical boundary in order to obtain a well-defined numerical system and to avoid the need to model the effects of air entrainment. However, it is a simple matter to add two plates in future experiments to match the numerical domain utilized here. The

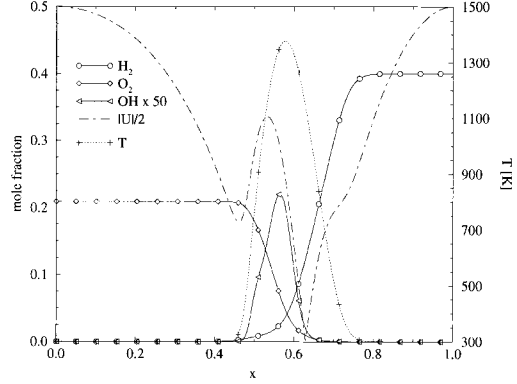


FIG. 2. Flame structure of the diffusion flame found along the axis of symmetry at $Re = 508.8$.

boundary conditions (at nozzle exits) were as follows: “parabolic” (and thus non-uniform) velocity profiles were prescribed at the exits of the fuel and oxidizer nozzles with equal peak velocities of 300 cm/s (corresponding to $Re = 508.8$ using the fluid properties of air at 300 K). Fuel consisted of 0.4 H_2 and 0.6 N_2 (by volume) at 300 K, while the oxidizer was air at 300 K. These physical parameters were chosen from one set of the experimental results reported in Ref. [1], in which multiple vigorously burning solutions and hysteresis were observed. In subsequent sections, all results are non-dimensionalized by the peak velocity of the airstream at the inflow boundary ($U_{air} = 300$ cm/s) and the diameter of the nozzles, D . Time is non-dimensionalized by $t_c = D/U_{air}$.

The steady-state two-dimensional diffusion flame from which we begin our calculations was first obtained as in Ref. [24]. We first simulated the mixing of fuel and oxidizer in the axisymmetric two-dimensional opposed-jet setup, then applied an ignition source and computed the entire ignition process until all transients died out and the steady two-dimensional diffusion flame (at $Re = 508.8$) was established.

Results and Discussion

We focus on two different steady solutions—a classical diffusion flame and an edge flame; both were obtained under identical conditions. The disk-shaped diffusion flame at $Re = 508.8$ is depicted in Fig. 1 (left column). Because of the small size of the nozzles, their close placement relative to one another, and the parabolic outflow velocity boundary condition, the strained diffusion flame considered here, strictly speaking, cannot be accurately described by the commonly used one-dimensional model [29,30]. The flame structure found along the axis of symmetry is shown in Fig. 2. This diffusion

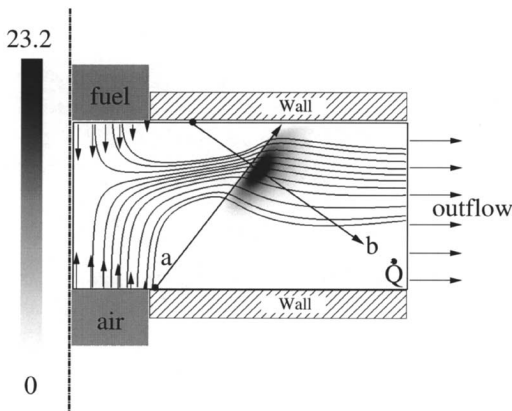


FIG. 3. Isocontours of the heat release rate, $(\Sigma_i \dot{\omega}_i H_i)/(\rho C_p)$, which is non-dimensionalized by t_c and 300 K; superimposed on this plot are the streamlines, the stoichiometric line, and two linear coordinates (lines a and b), along which the flame structures are extracted.

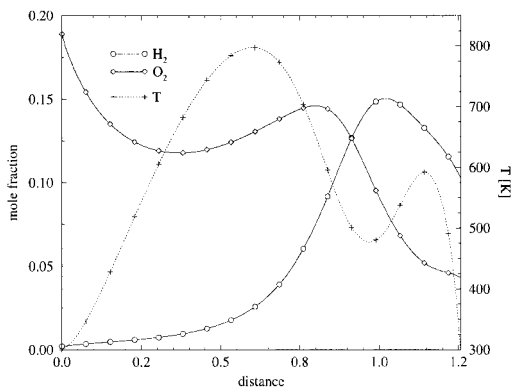


FIG. 4. Flame structure of the diffusion flame (temperature and mole fractions of H_2 and O_2) found along the front of the edge flame (along line a , as indicated in Fig. 3). Distance is non-dimensional.

flame was subjected to a near-extinction scalar dissipation rate; a further increase of the Reynolds number extinguished the flame in the region near the axis of the system. The transition Reynolds number agrees with what was reported in Ref. [1].

Starting with the steady diffusion flame obtained at $Re = 508.8$, the Reynolds number was increased to 700, and the diffusion flame disk was first extinguished in the vicinity of the axis of symmetry. An edge flame formed and propagated radially outward until it was stabilized at a certain radial position, forming a new steady flame. The stabilization mechanism seen here is aerodynamic in nature due to the divergence of the velocity field in the radial direction. Starting with this stable solution (an edge

flame) at $Re = 700$, the Reynolds number was decreased to $Re = 508.8$. The edge flame propagated back toward the axis (an ignition wave) but stabilized at a finite distance from the axis. The original disk shape diffusion flame did not recur even though the scalar dissipation rate had been decreased to its original subcritical level. Isocontours of velocity components, temperature, and the mole fractions of selected species of these steady flames are depicted in Fig. 1. The left column corresponds to the diffusion flame and the right column to the edge flame. Note that, for clarity, the numerical domain has been truncated in the radial direction in the figure.

Of interest is the structure of this edge flame, which propagates against the flow of a non-uniform mixture. In regions ahead of the edge flame, the mole fraction of H_2 varied in the range of 4%–17% (in the “preheat” region slightly ahead of the edge flame). To further analyze this edge flame, we plotted in Fig. 3 the isocontour of the heat release rate $((\Sigma_i \dot{\omega}_i H_i)/(\rho C_p))$ non-dimensionalized by $t_c/300$ K. We also plotted the streamlines and the stoichiometric line ($Z = Z_{st}$). Here, $Z = (\gamma Y_{H_2} - Y_{O_2} + Y_{O_2,air})/(\gamma Y_{H_2,fuel} + Y_{O_2,air})$, where γ denotes the stoichiometric ratio—that is, $\gamma = 1/2 W_{O_2}/W_{H_2}$ (W_i being the molecular weight of species i). The stoichiometric mixture fraction was $Z_{st} = 0.3892$ for the fuel and oxidizer compositions considered. Several interesting features can be seen in these figures:

1. The stoichiometric mixture fraction line does not go through the region where the heat release rate is at its maximum value. Instead, it passes near the cold wall, where chemical reaction is quenched and the edge flame only has a lean arm.
2. The slanted orientation of the edge flame and the leakage of hydrogen (marked by a circle in Fig. 1) are seen near the cold wall boundary. Hydrogen diffuses toward the high-temperature zone and is fully consumed in regions downstream of the edge flame. However, there is no discernible diffusion flame structure downstream of the edge flame.
3. The streamlines diverge as they approach the flame front (consistent with the results of Ref. [16]).

To further illustrate the flame structure, we extract cross sections (in directions “parallel” and “orthogonal” to the flame front) along the lines shown in Fig. 3. The origins (black dots) and directions of the one-dimensional coordinates on which the data are reported in Figs. 4 and 5 are also shown in Fig. 3. Fig. 4 is taken along the line approximately parallel to the edge flame in the preheat zone (line a in Fig. 3). The plots in Fig. 4 indicate clearly that the edge flame sees a mixture of hydrogen and air with strong variations in concentration along the direction parallel to the flame front. A rich mixture exists in the small region near the wall boundary on the fuel side

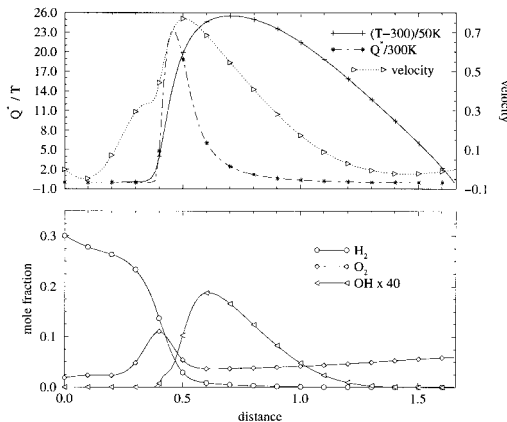


FIG. 5. Flame structure of the diffusion flame (temperature; mole fractions of H_2 , OH , and O_2 ; velocity projected on to the linear coordinate, and non-dimensional heat release rate) found orthogonal to the front of the edge flame (along line b , as indicated in Fig. 3). Distance is non-dimensional.

(the right edge in Fig. 4). However, the cold wall there quenches the flame.

The plots of temperature, species concentrations, and the velocity component orthogonal (projected along line b in Fig. 3) to the edge flame are reported in Fig. 5. Note that line b in Fig. 3 goes through the point where the heat release rate attains its maximum value, and, around this region, the plotted profiles in Fig. 5 resemble those of a premixed flame. However, far upstream and downstream of the reaction zone, the scalar profiles show significant variations reflecting the two-dimensional nature of this edge flame. For example, it can be seen that, downstream of the reaction zone, O_2 concentration rises and temperature drops due to transport in the transverse direction. The propagation velocity of the edge flame (taken to be the velocity of the flow ahead and in a direction orthogonal to the flame front) is about 105 cm/s, which agrees well with that of a lean H_2 /air mixture [31].

The edge flame is responsible for the hysteresis reported in Ref. [1]. After the diffusion flame disk is extinguished, an edge flame that has the characteristics of a premixed flame forms. This edge flame stabilizes itself at a location where the incoming flow velocity matches the local propagation velocity. To recover the initial contiguous diffusion flame (*contiguous* refers to a simply connected flame as opposed to one with a hole), one has to reduce the flow rate such that the local propagation velocity of this edge flame exceeds the local flow velocity to allow it to propagate all the way back to the axis of symmetry. Reducing the flow rate to produce a subcritical strain rate alone is not sufficient to ensure that a contiguous diffusion flame can be recovered.

Conclusions

Using detailed chemistry and realistic transport, we performed direct numerical simulations to explain the transition between two different vigorously burning flame configurations observed in a recent experiment. We found two stable solutions that explain the multiple solutions described briefly in Ref. [1]. Our DNS results revealed the nature of the second solution: it is an edge flame that propagates against a stream of non-uniform mixture in the opposed-jet configuration. The hysteresis observed in the experiment can be explained by the propagation of the edge flame. This hysteresis is different from those associated with the classical S-shaped curve: for the same value of the Reynolds number, two solutions corresponding to vigorously burning flames coexist with the pure mixing (or weakly burning flame) solution. It may also be important in improving our understanding of the local reignition in a turbulent flame brush, in that the reduction of the local strain rate to the subcritical level may not be sufficient for the diffusion flame to re-establish due to the propagation character of the edge flame. The local velocity field has to allow the propagation of this edge flame to reignite the mixture and re-establish the contiguous diffusion flame. Future work will aim at utilizing an arc-length continuation method to compute the solution branches of this transition phenomenon and to construct experiments that match the numerical system more closely. Lastly, the agreement between the numerical results and what was observed in the experiment suggests that the traditional opposed-jet experimental setup can be used as a device to study edge flames. One clear advantage of this setup is that the system is strictly two-dimensional, making it possible to have matching detailed numerical simulations to complement the experimental endeavor.

Acknowledgments

This work was performed with the financial support of the Swiss National Science Foundation and the Swiss Office of Energy.

REFERENCES

1. Pellet, G. L., Isaac, K. M., Humphreys Jr., W. M., Gartrell, L. R., Roberts, W. L., Dancy, C. L., and Northam, G. B., *Combust. Flame* 112:575–592 (1998).
2. Tomboulides, A. G., Lee, J. C. Y., and Orszag, S. A., *J. Sci. Comput.* 12(2):139–167 (1997).
3. Potter, A. E., and Butler, J. N., *ARS J.* 29:54:54–56 (1959).
4. Schefer, R. W., and Goix, P. J., *Combust. Flame* 112:559–574 (1988).
5. Peters, N., *Proc. Combust. Inst.* 21:1231 (1986).

6. Buckmaster, J., *J. Eng. Math.* 31:269–284 (1997).
7. Wichman, I. S., *Prog. Energy Combust. Sci.* 18:553–593 (1992).
8. Buckmaster, J., Jackson, T. L., and Yao, J., *Combust. Flame* 117:541–552 (1999).
9. Buckmaster, J., and Weber, R., *Proc. Combust. Inst.* 26:1143–1149 (1996).
10. Muñoz, L., and Mungal, M. G., *Combust. Flame* 111:16–31 (1997).
11. Shay, M., and Ronny, P., *Combust. Flame* 112:171–180 (1998).
12. Vervisch, L., and Poinso, T., *Annu. Rev. Fluid Mech.* 30:655–691 (1998).
13. Dold, J. W., *Combust. Flame* 76:71–88 (1989).
14. Hartley, L. J., and Dold, J. W., *Combust. Sci. Technol.* 80:23–46 (1991).
15. Kioni, P. N., Rogg, B., Bray, K. N. C., and Liñán, A., *Combust. Flame* 95:276–290 (1993).
16. Ruetsch, G. R., Vervisch, L., and Liñán, A., *Phys. Fluids* 7:1447–1454 (1995).
17. Echekki, T., and Chen, J., *Combust. Flame* 114:231–245 (1998).
18. Im, H. G., and Chen, J. H., *Combust. Flame* 119:436–454 (1999).
19. Azzoni, R., Ratti, S., Aggarwal, S. K., and Puri, I. K., *Combust. Flame* 119:23–40 (1999).
20. Plessing, T., Terhoeven, P., and Peters, N., *Combust. Flame* 115:335–353 (1998).
21. Tomboulides, A. G., “Direct and Large-Eddy Simulations of Wake Flow: Flow Past a Sphere,” Ph.D. thesis, Princeton University, Princeton, NJ, 1993.
22. Tomboulides, A. G., and Orszag, S. A., *J. Comput. Phys.* 146(2):691–706 (1998).
23. Lee, J. C., Tomboulides, A. G., Orszag, S. A., Yetter, R., and Dryer, F. L., *Proc. Combust. Inst.* 26(2):3059–3065 (1996).
24. Frouzakis, C. E., Lee, J. C., Tomboulides, A. G., and Boulouchos, K., *Proc. Combust. Inst.* 27(1):571–577 (1998).
25. Brown, P. N., Byrne, G. D., and Hindmarsh, A. C., *SIAM J. Sci. Stat. Comput.* 10(5):1038–1051 (1989).
26. Hindmarsh, A. C., *ODEPACK: A Systematized Collection of ODE Solvers*, Scientific Computing, IMACS, North-Holland Publ., 1983, pp. 55–64.
27. Yetter, R. A., Dryer, F. L., and Rabitz, H., *Combust. Sci. Technol.* 79:97–128 (1991).
28. Coffee, T. P., and Heimerl, J. M., *Combust. Flame* 50:323–340 (1983).
29. Kee, R. J., Miller, J. A., Evans, G. H., and Dixon-Lewis, G., *Proc. Combust. Inst.* 22:1479–1494 (1988).
30. Lutz, A. E., Kee, R. J., Grcar, J. F., and Rupley, F. M., *OPPDIF: A FORTRAN Program for Computing Opposed-Flow Diffusion Flames*, Sandia report SAND96-8243 UC-1409.
31. Glassman, I., *Combustion*, 2nd ed., Academic Press, London 1987, p. 460.

COMMENTS

Jaideep Ray, Sandia National Labs, USA. Did you observe the tribrachial flame in both the one-step and H_2/O_2 cases? Also, if you plotted the fuel consumption rate of the tribrachial configuration, was it symmetrical about the stoichiometric line?

Author's Reply. We did not perform calculations of H_2/O_2 flames with one-step chemistry. In our earlier paper [1], the calculation which showed tribrachial flame structure utilized a fictitious fuel/oxidizer system with one-step chemistry and simplified transport. The transport properties and the stoichiometry (1:1) there does not correspond to the H_2/O_2 system; it was merely a generic reactive system used to illustrate our numerical approach which was new at the time. Nevertheless, when we changed the Damköhler number, this generic system (on an opposed-jet configuration) changed from the traditional diffusion flame

disk to a tribrachial flame structure. Because of the simplification adopted in this earlier work, the tribrachial flame was completely symmetrical on both the fuel and oxidizer sides (all thermodynamic properties of the fuel and oxidizer are identical and the mass fractions of both reactants streams are equal to one at the nozzle exits). We would like to note that in this simple calculation, when the stoichiometry was changed from 1 to 0.5, the tribrachial flame becomes slanted in much the same way as the H_2/O_2 edge flame shown in the realistic simulation reported in the current endeavor.

REFERENCE

1. Tomboulides, *JSC* 12(2):139–167 (1997).